Colloid Polym Sci (2009) 287:561–568
DOI 10.1007/s00396-009-2003-6

ORIGINAL CONTRIBUTION

Semicontinuous microemulsion copolymerization of vinyl acetate and butyl acrylate: high solid content and effect of monomer addition rate

Víctor M. Ovando-Medina · René D. Peralta · Eduardo Mendizábal

Received: 21 October 2008 / Revised: 4 January 2009 / Accepted: 9 January 2009 / Published online: 7 February 2009

Abstract Vinyl acetate and butyl acrylate were copolymerized in microemulsion under monomer-starved conditions by a semicontinuous process using different monomer addition rates (R_a). A mixture of sodium dodecyl sulfate and polyethylene glycol dodecyl ether (Brij®35) were used as surfactants. Potassium persulfate was the initiator. High copolymer content latexes (around 40 wt.%), average particle diameters (D_p)<50 nm and polymer-to-surfactant ratios (12 to 14, weight/weight) were obtained with weight average molar masses (M_w) between 180,000 and 760,000. D_p and M_w of the copolymers decrease as R_a is decreased. As R_a increases, a shoulder in the molar mass distribution was observed at high values of M_w, which was ascribed to chain transfer to polymer. Homogeneous copolymer compositions were observed throughout the reaction, which cannot be obtained by the usual batch process.

Keywords Microemulsion copolymerization · Vinyl acetate · Butyl acrylate · Semicontinuous · Monomer-starved

Introduction

Microemulsions are thermodynamically stable systems which are formed spontaneously by mixing an organic and an aqueous phase in the presence of a surfactant in the proper amounts [1]. By microemulsion polymerization, it is possible to obtain polymeric nanoparticles with diameters (D_p) <50 nm and polymers with high molar mass and a variety of microstructures, which influence polymer properties [2]. In microemulsion polymerization, it is necessary to use a large amount of surfactant to stabilize the polymer particles during polymerization and storage. Usually, the microemulsion polymerization process yields microlatexes with low polymer content and low polymer to surfactant ratio, which makes the process nonsuited for practical applications [3]. To overcome these difficulties, some strategies have been developed: polymerizations in Winsor I-like systems (*o*/*w* microemulsion in equilibrium with an upper oil layer), the use of surfactants with high monomer solubilization capacity (which increases the microemulsion region), and the polymerization in semicontinuous regimes [3–13].

Because of the high surfactant content employed in the batch microemulsion polymerization process, void micelles present in the final latex can be refilled with monomer (semicontinuous process) to continue particle nucleation to obtain a latex with high polymer content (>30%) with particles sizes in the range obtained in the batch process. Previously reported works in semicontinuous microemulsion polymerization have been mainly on homopolymerizations, and they were aimed to surfactant optimization and to increase the polymer content in the final latex. Ramírez et al. [13] studied the effect of potassium persulfate (KPS) on particle formation of poly(butyl acrylate) in semicontinuous polymerization of seeded microemulsions using a mixture

V. M. Ovando-Medina
Departamento de Ingeniería Química,
Coordinación Académica Región Altiplano (COARA)
Universidad Autónoma de San Luis Potosí,
Carretera a Cedral KM 5+600, San José de las Trojes,
Matehuala, San Luis Potosí 78700, México

R. D. Peralta
Centro de Investigación en Química Aplicada (CIQA),
Blvd. Enrique Reyna Hermosillo # 140,
Saltillo, Coahuila 25253, México

E. Mendizábal (✉)
Centro Universitario de Ciencias Exactas e Ingeniería,
Departamento de Química, Universidad de Guadalajara,
Blv. M. García Barragán #1451,
Guadalajara, Jalisco 44430, México
e-mail: lalomendizabal@hotmail.com

Table 1 Recipes used in the microemulsion copolymerizations of VAc and BuA

Run	A		B		C		D	
Component	Batch	SC	Batch	SC	Batch	SC	Batch	SC
H_2O (g)	94.0		94.0		94.0		94.0	
SDS (g)	3.03		3.03		3.03		3.03	
Brij®35 (g)	1.015		1.015		1.015		1.015	
KPS (g)	0.061		0.061		0.061		0.061	
VAc (g)	2.568	51.0	2.618	51.0	2.605	51.0	2.605	51.0
BuA (g)	0.462	9.10	0.462	9.10	0.462	9.10	0.462	9.10
R_a (g/min)		0.10		0.20		0.30		0.50

SC semicontinuous

of sodium dodecyl sulfate (SDS) with Aerosol OT as the surfactants. The resultant lattices contained particles with D_p<40 nm, polymer contents close to 30 wt.%, and polymer to surfactant ratio, *P*/*S*, of 20:1 (wt./wt.). They reported that D_p increases with increasing initiator concentration. These authors divided the polymerization process in three periods: batch polymerization (in which a small fraction of the total monomer in the recipe is polymerized), semicontinuous addition, and the post-addition period. In the batch period, they observed that D_p reaches a maximum from which it starts to decrease, while the particle number density (N_p) increases. Throughout the semicontinuous period, D_p and N_p increase, and during the postaddition period, D_p continues growing, while N_p decreases due to particle coagulation because when monomer addition is completed, the system tends to reduce its free energy. The authors concluded that the monomer concentration in the aqueous phase is a key factor in the formation of particles. Xue and coworkers [14] studied the effects of monomer addition rate on the polymerization rate (R_p) and on the molar masses in the modified microemulsion polymerization of methyl methacrylate using SDS as surfactant and KPS or redox systems as initiators. They achieved polymer contents of 10 to 30 wt.%, whereas D_p values were in the range of 20 to 40 nm. Furthermore, they observed that R_p and molar masses increase with R_a.

Table 2 Final characteristics of the latexes

Run	$M_w \times 10^{-5}$ (g/mol)	PDI	$N_p \times 10^{-17}$	P.C. (wt.%)	*P*/*S*
A	1.8	5.3	11.5	38.4	14.2
B	3.0	4.4	9.9	40.0	14.6
C	2.7	4.0	9.3	39.1	14.0
D	7.6	5.5	9.6	37.8	13.4

PDI Polydispersity index, M_w/M_n; *P.C.* polymer content; *P/S* polymer to surfactant ratio, wt./wt

In this work, the effects of monomer addition rate on the kinetics, particle size, copolymer molar mass, and composition in the semicontinuous microemulsion copolymerization of vinyl acetate and butyl acrylate are reported. Also, we report the preparation of microlatex with low surfactant concentration containing particles with diameter (D_p) less than 50 nm and solid content around 40 wt.%, content which is much higher than previously reported values for microemulsion polymerization. The comonomer pair vinyl acetate and butyl acrylate are widely used in industry for the preparation of poly(vinyl acetate-*co*-butyl acrylate) latexes that find applications in coating formulations. Besides, their wide difference in reactivity ratios and in water solubility makes it difficult to obtain copolymers with homogeneous composition and represent an interesting challenge to study its preparation in microemulsion polymerization under monomer-starved conditions as was selected for this investigation.

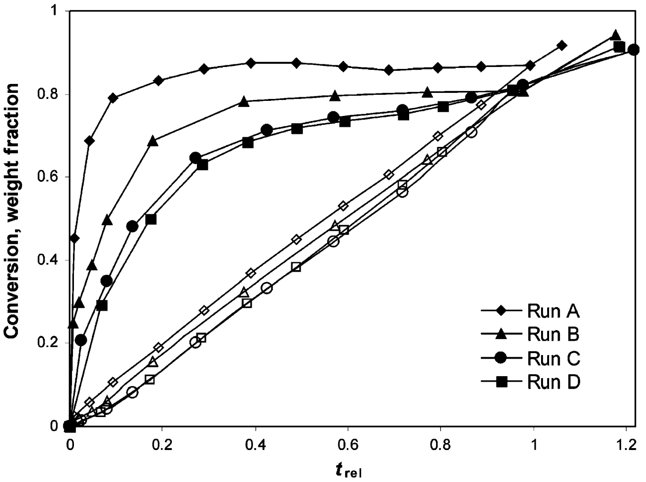

Fig. 1 Instantaneous (*filled symbols*) and global (*empty symbols*) conversions as a function of the relative time (t_{rel}), at different monomer mixture addition rates (R_a)

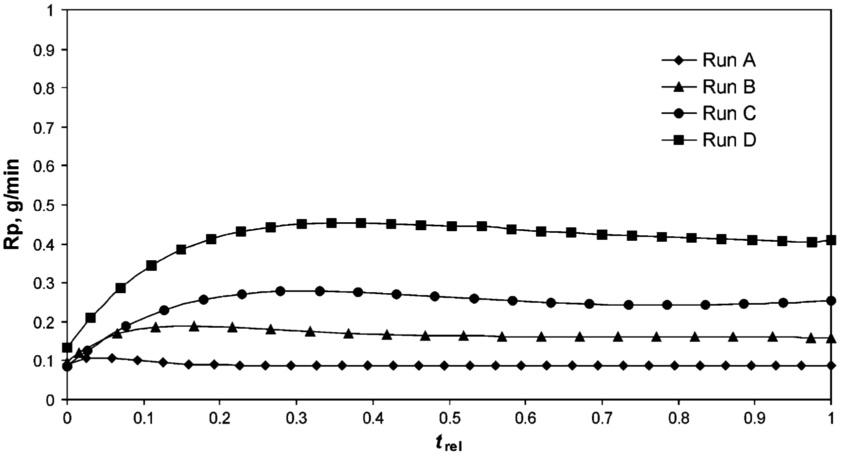

Fig. 2 Overall polymerization rate (R_p) vs. relative time for the different monomer addition rates

Experimental

Materials

Vinyl acetate (VAc), butyl acrylate (BuA), KPS, hydroquinone, and Brij®35 (polyethylene glycol dodecyl ether) were purchased from Aldrich (≥99%); SDS was from Fluka (≥99%). VAc was washed with a 2 N NaOH aqueous solution and dried with $CaCl_2$ and $MgSO_4$ during 12 h and subsequently vacuum distilled at 40 °C. BuA was dried with $CaCl_2$ and vacuum distilled at 40 °C. All the other reactants were used as received. Deionized, tridistilled grade water (obtained from a system of two ionic-interchange columns, Cole–Parmer Instruments) and argon of ultrahigh purity from Infra were used. Tetramethylsilane from Aldrich was used as internal reference in proton nuclear magnetic resonance (^{1}H-NMR) analyses.

Copolymerizations

The one-phase *o*/*w* microemulsions at 60 °C were determined visually by titrating aqueous micellar solutions of a mixture of SDS: Brij®35 (3:1 wt./wt.) with the monomer mixture VAc/BuA (85:15 wt./wt.). The microemulsión composition selected for polymerization is shown in Table 1 (batch column). The recipes and reaction conditions are given in Table 1. The polymerizations were initiated in batch mode in a 250-mL glass-jacketed reactor equipped with magnetic stirring. The surfactant mixture and water were charged to the reactor, cooled to 0 °C and vacuum degassed, and then the system was saturated with argon. The reactor was heated to 60 °C, and a fraction of the oxygen-free monomer mixture saturated with argon was added to the reactor. Then, a KPS solution (2 wt.% with respect to the monomer mixture) was added in one shot to initiate the polymerization (batch period). After 4.5 min of initiating the reaction, the oxygen-free monomer mixture was added continuously to the reactor using a gas-tight syringe (Hamilton GASTIGHT®) adapted to a calibrated addition pump (Kd-Scientific®). After the semicontinuous addition period, the reactions were allowed to continue for 30 min. Conversion was followed gravimetrically: samples were withdrawn from the reacting system at given times and placed in vials (of known weight) immersed in an ice

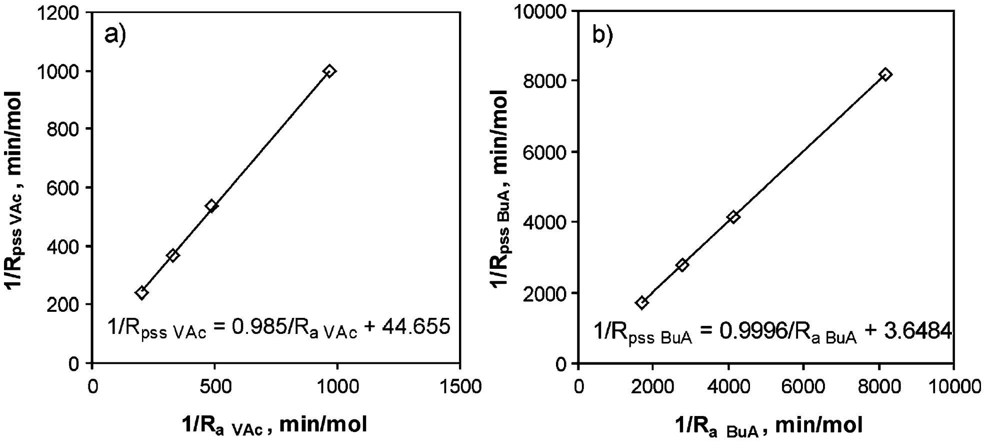

Fig. 3 Reciprocal of the polymerization rate vs. the reciprocal of monomer addition rate at the PSS. **a** Vinyl acetate, **b** butyl acrylate

Fig. 4 Average particle diameter as a function of time at different R_a

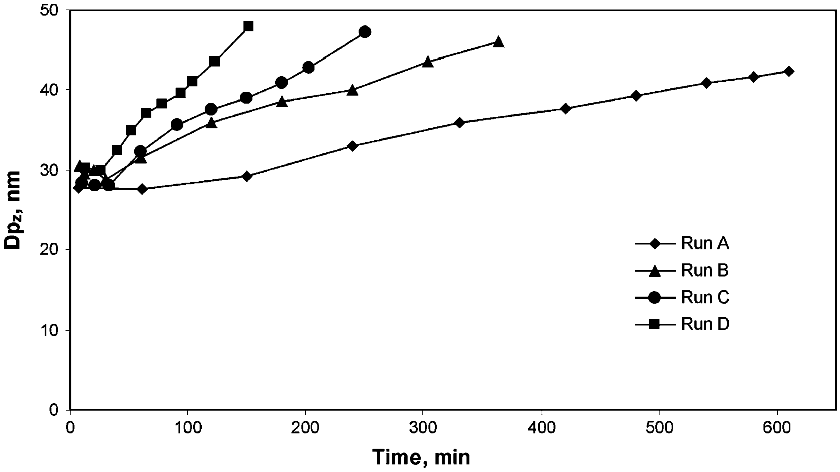

bath containing 0.5 g of an aqueous hydroquinone solution (0.4 wt.%). Then, the samples were weighed and freeze dried (Labconco Freeze Dry System/R45). The weight of polymer was estimated by subtracting the known weights of surfactants and hydroquinone from the total weight of the freeze-dried samples.

Characterization

Particle size was measured in a Malvern 4700 quasielastic light-scattering (QLS) apparatus equipped with an argon laser (λ=488 nm). Measurements were performed at 25 °C at an angle of 90°. Copolymer samples were washed with hot water (to remove the surfactants) and vacuum dried for 24 h. Copolymer compositions were determined by ^{1}H-NMR in an FTNMR Gemini 200 Varian apparatus (200 MHz), using 10 mg/mL sample solutions in chloroform-*d*. Average molar masses and molar mass distributions (MMD) of copolymers were determined in a Hewlett-Packard series 1100 gel permeation chromatograph equipped with a refractive index detector and using high-performance liquid chromatography-grade tetrahydrofurane (Aldrich) as mobile phase. Because polystyrene standards were used, for correction of the gel permeation chromatography results, the weighted averages of the parameters in the Mark–Houwink equation, α and K, were calculated using the cumulative copolymer composition (obtained previously by ^{1}H-NMR spectrometry) following the procedure reported by Jovanovic and Dubé [16].

Results

From previous experiments in batch mode, it was found that the maximum polymerization rate occurs around 4.5 min after reaction initiates. Then, to allow seed formation and to have monomer-starved conditions when feeding starts, all the runs were carried out in batch mode for 4.5 min, and the continuous addition of the monomers was started at the end of this period. The originally clear and translucent microemulsions turn bluish and opaque upon polymerization, indicating the start of the reaction. As

Fig. 5 Particle size distribution obtained by QLS at different monomer addition rates and conversions: addition rate **a** 0.10 g/min; **b** 0.50 g/min

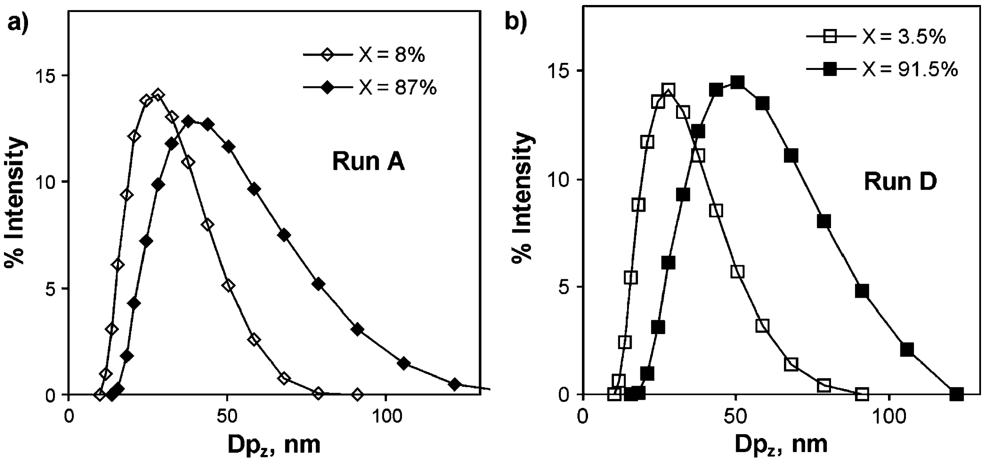

more monomer reacts, the reaction mixture turns more opaque as a consequence of the growing polymer particles and increased monomer conversion. The final characteristics of the latexes and copolymers obtained in the semicontinuous copolymerization of VAc and BuA (85:15 wt./wt.) at 60 °C are shown in Table 2, where it can be seen that microlatex with very high polymer content (around 40 wt.%) and high *P*/*S* ratios (~14) were obtained.

Figure 1 shows the instantaneous (x) and global (X) conversions as a function of the relative time, t_{rel}, at different monomer mixture addition rates (R_{a}), as detailed in Table 1. The relative time was defined as the ratio of the sampling time to the total addition time. Because the monomer addition rates are different, time was normalized to compare the polymerizations at the same amount of added monomer. Global conversion is given by the amount of copolymer formed at time t divided by the total amount of monomers added. In Fig. 1, it can be observed that the instantaneous conversion increases as R_{a} is decreased and the polymerization time required to reach a constant x value decreases. When the monomer addition is stopped, the reaction continues for 30 min, and in all cases, a final global conversion (X) of ca. 95% was obtained.

Figure 2 shows that, after $t_{\mathrm{rel}}\approx 0.3$, the overall polymerization rate (R_{p}) is practically constant, and if R_{a} is increased, higher R_{p} values are obtained. In our case, the overall polymerization rate was obtained by taking the derivative of the equation for the global conversion $\left(X = \left[M_0 + \left(t - t_{\mathrm{pp}}\right)R_{\mathrm{a}}\right]x/M_{\mathrm{tot}}\right)$ with respect to time; where t_{pp} corresponds to the time of the batch polymerization period; R_{a}, M_0, and x represent the monomer addition rate, initial amount of monomers charged to the reactor, and instantaneous conversion, respectively. M_{tot} is the total amount of monomers added. Therefore, R_{p} can be expressed by $R_{\mathrm{p}} = (M_{\mathrm{tot}})\mathrm{d}X/\mathrm{d}t = \left[M_0 + \left(t - t_{\mathrm{pp}}\right)R_{\mathrm{a}}\right]\mathrm{d}X/\mathrm{d}t + xR_{\mathrm{a}}$.

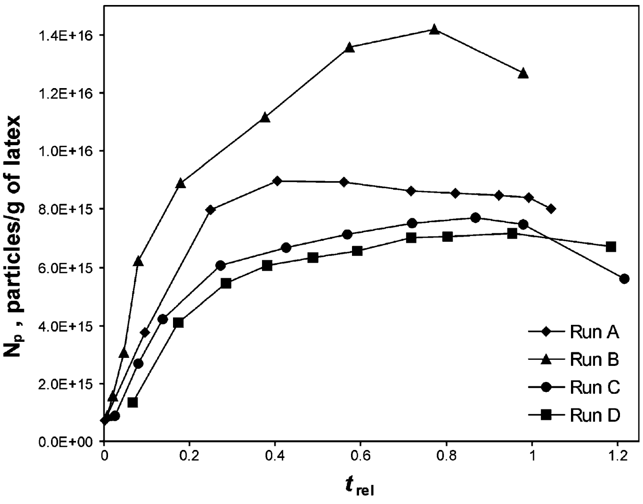

Fig. 6 Number of particles, N_{p}, as a function of time

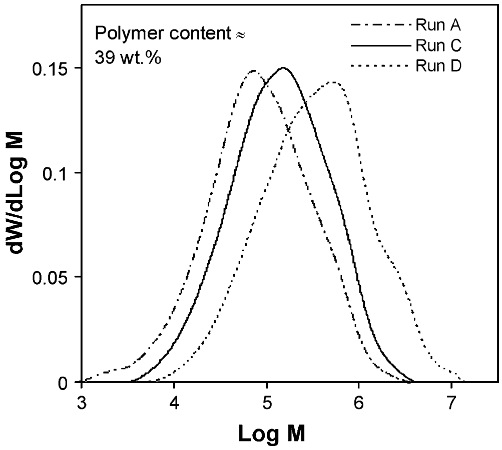

Fig. 7 Molar mass distributions of the copolymers at the end of reaction

The interval where R_{p} is constant is known as the pseudosteady state stage (PSS) of the reaction rate [17]. If the monomer addition rate is enough to maintain the monomer saturation concentration in the polymer particles, R_{p} becomes independent of R_{a} (flooded region). However, if the monomer concentration in the polymer particles falls below this value, R_{p} approaches a constant value which depends on R_{a} (monomer-starved conditions) [18].

Dimitratos et al. [18] showed that, for emulsion copolymerizations in the PSS under starved conditions, R_{p} is related to R_{a} as follows:

$$1/R_{\mathrm{p}i} = 1/\dot{K}_i + C_i/R_{\mathrm{a}i} \tag{1}$$

$\dot{K}_i$ is a constant which indicates the capacity of the system to consume monomer i and is proportional to the number of particles, to the average radicals per particle, and to the propagation rate coefficients; c_i is a constant which is theoretically equal to 1.

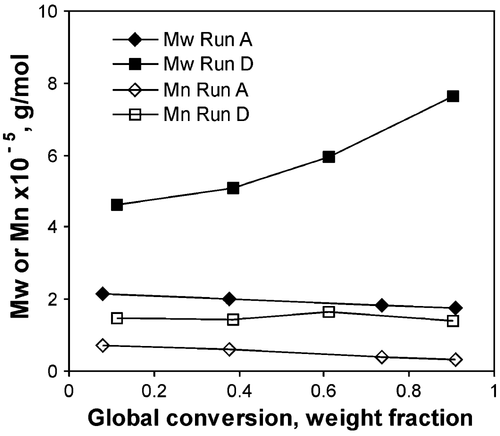

Fig. 8 Average molar masses (M_{n} and M_{w}) as a function of global conversion obtained at different monomer addition rates

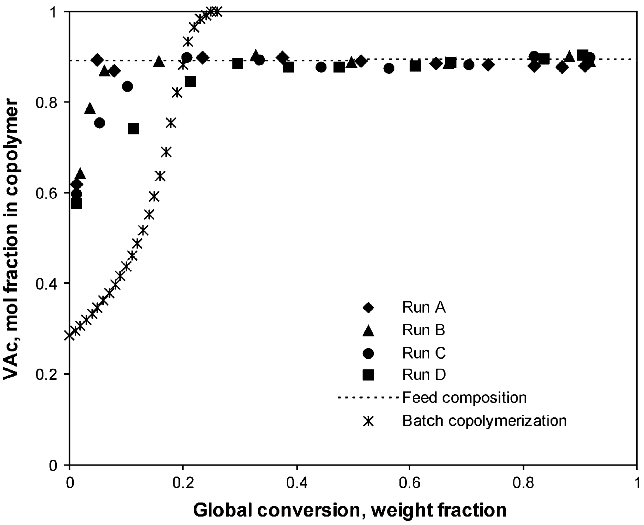

Fig. 9 Instantaneous copolymer composition as a function of global conversion for semicontinuous and batch microemulsion copolymerizations

The polymerization rate of monomer i, R_{pi}, was calculated using Eq. 2:

$$R_{pi} = \left[R_{ai}\left(t - t_{pp}\right) + M_{0i}\right]\frac{dx_i}{dt} + R_{ai}x_i \qquad (2)$$

Where R_{ai}, M_{0i}, and x_i represent the addition rate of monomer i (mol/min), initial amount of monomer i charged to the reactor (mol) and instantaneous conversion of monomer i (VAc or BuA), respectively. Experimental copolymer compositions were used to calculate the instantaneous conversion of each monomer, following the procedure reported by Delgado [19]. From Fig. 3, the K_i and c_i values were obtained and compared with those reported by Dimitratos et al. [18] for the emulsion copolymerization of the same monomers.

The evolution of the average particle diameter as a function of time at different R_a is shown in Fig. 4. D_p increases with conversion, and as R_p increases, the particles grow faster. In Fig. 5, the particle size distributions (PSD) at two different monomer addition rates and conversions are shown. As reaction progresses, the PSDs broaden and are shifted to higher particle sizes. Figure 6 shows the number density of particles, N_p, as a function of relative time. N_p increases continuously as monomer is added, and when monomer addition is stopped, N_p decreases slightly due to particle coagulation.

The molar mass distributions of the copolymers at final conversions are depicted in Fig. 7, where a shoulder at high molar masses is observed. Also, it can be seen that this shoulder is more pronounced, and the MMDs are displaced to higher molar masses as R_a is increased. The polydispersity indexes of the final copolymers varied between 4.0 and 5.5.

In Fig. 8, the evolution of the number average molar mass, M_n, and the weight average molar mass, M_w, for the lower and higher values of R_a are shown. For the lower R_a employed, M_w and M_n decrease slightly throughout the reaction, and for the higher R_a, M_n remains almost constant, while M_w increases during the reaction.

In Fig. 9, the evolution of instantaneous copolymer composition obtained in the semicontinuous process is compared with the results reported elsewhere for the batch polymerization of the same monomers [15]. It is clear that by the semicontinuous process it is possible to obtain a more homogeneous copolymer composition.

Discussion

It has been reported that, when using ionic surfactants, the critical micellar concentration decreases by the incorporation of a small amount of non-ionic surfactant [20]. Then, to obtain a large microemulsion zone using a low surfactant

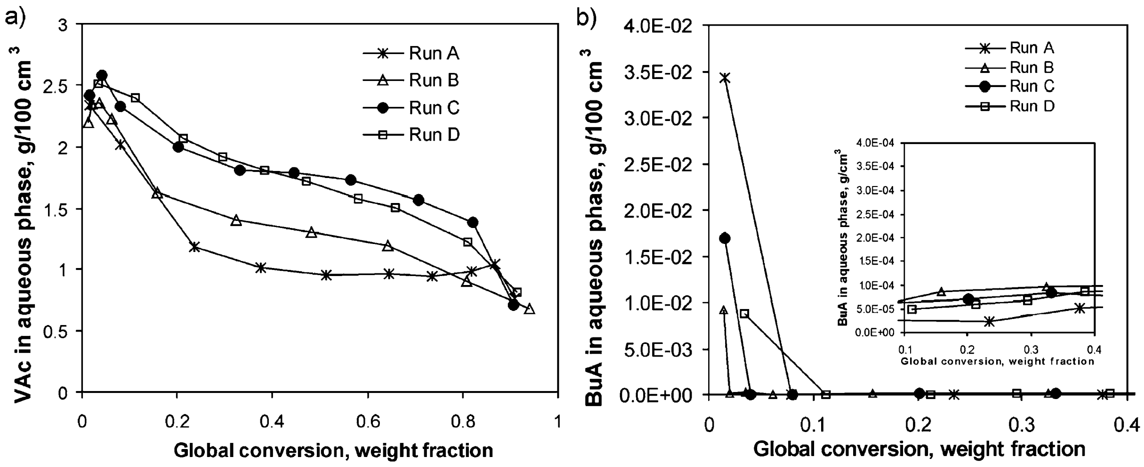

Fig. 10 Monomer concentration in the aqueous phase as a function of global conversion. **a** Vinyl acetate, **b** butyl acrylate

Table 3 $\dot{K}_i$ and c_i values obtained by steady state analysis of experimental

Monomer	$\dot{K}_i$[a] (mol/min)	c_i[a]	$\dot{K}_i$[b] (mol/min)	c_i[b]
VAc	0.022	0.99	0.03	1.04
BuA	0.274	1.0	0.1	1.0

[a] This work

[b] Reported in [17]

concentration, a combination of ionic and non-anionic surfactant was used. In previous experiments, we tested five surfactant systems trying to find a combination of anionic and non-ionic surfactants that gave the widest microemulsion region while keeping a low proportion of these components. The mixture of SDS/Brij®35 (3:1) met the requirements.

When the monomer concentration in the continuous phase (aqueous) is below the saturation value, it is not possible to obtain particles saturated with monomers, and the system is under monomer-starved conditions [21]. In this work, the monomer concentrations in the aqueous phase and polymer particles were estimated using thermodynamic equilibrium equations combined with mass balances [15, 22, 23]. Figure 10a, b show the concentrations of each monomer in the aqueous phase. At the beginning of reaction, the monomer concentrations in the aqueous phase are approximately 2.39 g of VAc/100 cm^3 and 0.03 g of BuA/100 cm^3, and these concentrations decrease as polymerization proceeds, giving as a result that monomer concentrations are always below their water saturation value, (2.5 g of VAc/100 cm^3 and 0.14 g of BuA/100 cm^3); then, in all cases, the polymerizations took place under monomer-starved conditions. In semicontinuous heterogeneous polymerizations under monomer-starved conditions, particle nucleation predominates over particle growth [24, 25]. In all cases, new particles are formed throughout the reaction (Fig. 6), and although particle size increases with conversion (Fig. 4) at the end of reaction, they are in the range of microemulsion-made particles.

High instantaneous conversions, x, were obtained since almost the beginning of reaction, and they become higher when decreasing R_a (Fig. 1). A decrease in x when R_a increases has been reported in semicontinuous emulsion and microemulsion polymerization under monomer-starved conditions [17, 26]. Table 2 shows that latexes with high solid content, low surfactant amount and small particles were obtained, which is an important result for this process to be used at industrial level even though the surfactant would have to be removed for some applications.

Table 3 shows that the c_i values are similar to the theoretical value. Because the $\dot{K}_i$ value depends on factors such as number of particles in the system, average number of radicals per particle, propagation rate constants, and others [18], the $\dot{K}_i$ values obtained here differ from the values reported in the emulsion polymerization of the same monomers.

For a polymerization process in a semicontinuous regime under monomer-starved conditions, the instantaneous particle growth rate, $\mu(t)$ is given by [27]:

$$\mu(t) = \frac{R_a}{N_p} \tag{3}$$

Equation 3 predicts an increase in $\mu(t)$ when the rate of monomer addition increases and the particle density number decreases. This is confirmed in Fig. 4 where it can be observed that D_p increases faster when R_a increases and the number density of particles decreases (Fig. 6). Because in the semicontinuous polymerization process the particle formation period is forced to extend for a longer time compared with a batch process, the particles formed at the onset of the polymerization grow to a greater extent than particles formed thereafter, giving as a result a particle size distribution skewed toward bigger particles, as observed in Fig. 5.

In batch microemulsion polymerization, bimolecular termination is almost absent because of the compartmentalization effect, and as a consequence, M_w is high because transfer to monomer is the dominant mechanism for termination of chain growth. Table 2 shows that, in semicontinuous microemulsion polymerization under monomer-starved conditions, much lower molar masses (<1,000,000) are obtained than in batch (>1,500,000). Table 2 also shows that the molar masses are displaced toward lower values as R_a decreases. It has been reported [14, 28, 29] that under monomer-starved conditions when the monomer feed rate decreases the amount of monomer inside the particles also decreases. At low monomer content, k_p decreases substantially due to the glass effect [30]. Because of these factors, there is a large decrease in R_p (Fig. 2) giving as a result that there is enough time for the entry of a radical to the particle to stop chain growth before attaining high molar mass [31].

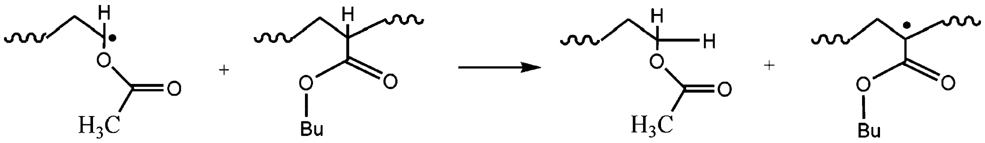

Fig. 11 Subtraction of tertiary H atoms from the copolymer BuA units by a VAc reactive chain end [32]

In Fig. 7, the molar mass distributions of the final latexes show a high molar mass population (a shoulder in the MMD around 3×10^6 Da) which can be explained by chain transfer to polymer. Britton et al. [32] studied the degree of branching in the semicontinuous emulsion copolymerization of VAc and BuA and found a synergistic effect in which small quantities of one of the monomers produces a dramatic increase in the degree of branching. This branching results in the subtraction of tertiary H atoms of the copolymer BuA units by a VAc-reactive chain end (Fig. 11). The same authors found that chains with a reactive VAc end subtract H atoms from the BuA units seven to eight times faster than from VAc units; they also found that radicals with a VAc reactive end are three to four times more effective in the subtraction of H atoms from BuA repetitive units than radicals with a BuA reactive end.

Because of the great difference in water solubility and in reactivity ratios between BuA and VAc, it is not possible to obtain copolymers of homogeneous composition by batch microemulsion or emulsion copolymerization [33]. Figure 9 shows that under semicontinuous conditions, instantaneous copolymer composition close to the feed composition was obtained through the reaction, and the lower the R_a used the more homogeneous the copolymer composition. Whereas the copolymer obtained by batch polymerization [15] showed a high drift in composition and at global conversions larger than 0.2, practically only poly(vinyl acetate) homopolymer is formed.

Conclusions

By the semicontinuous microemulsion copolymerization of VAc and BuA under monomer-starved conditions, it is possible to obtain latexes containing particles with average diameters smaller than 50 nm, polymer to surfactant ratios from 12 to 14, weight/weight with copolymer content around ~40 wt.%, which is much higher than reported values for microemulsion polymerization, and copolymers with homogeneous composition (copolymer composition close to the feed co-monomer composition) which cannot be obtained by batch copolymerization for the VAc/BuA comonomer pair.

Small high molar mass populations were observed in the MMD, which can be explained by chain transfer to polymer.

By the copolymerization process reported here, it is possible to control particle size, copolymer composition, and molar mass by modifying the monomer mixture addition rate (R_a).

Acknowledgments This work was supported by the Consejo Nacional de Ciencia y Tecnología, México (grants # SEP-2003-C02-44811/A-1 and CB-61345).

References

1. Shi Y, Wu Y, Hao J, Li GJ (2005) Polym Sci Part A: Polym Chem 43:203
2. Herrera JR, Peralta RD, López RG, Cesteros LC, Mendizábal E, Puig JE (2003) Polymer 44:1795
3. Sosa N, Peralta RD, López RG, Ramos LF, Katime I, Cesteros C, Mendizábal E, Puig JE (2001) Polymer 42:6923
4. Gan LM, Lian N, Chew CH, Li GZ (1994) Langmuir 10:2197
5. Loh SE, Gan LM, Chew CH (1996) J Macromol Sci Pure Appl Chem A 33:371
6. Xu X, Fei B, Zhang Z, Zhang MJ (1996) Polym Sci: Part A: Polym Chem 34:1657
7. Xu X, Zhang Z, Wu H, Ge X, Zhang M (1998) Polymer 39:5245
8. Xu XJ, Chew CH, Siow KS, Wong MK, Gan LM (1999) Langmuir 15:8067
9. Rabelero M, Zacarias M, Mendizábal E, Puig JE, Dominguez JM, Katime I (1997) Polym Bull 38:695
10. Roy S, Devi S (1997) Polymer 38:3325
11. Ming W, Jones FN, Fu S (1998) Macromol Chem Phys 199:1075
12. Ming W, Jones FN, Fu S (1998) Polym Bull 40:749
13. Ramírez AG, López RG, Tauer K (2004) Macromolecules 37:2738
14. Xue Y, Jiang W, Zhao Y, Yang W, Fu S, Vormerg LJ (2005) Macromol Sci Part A: Pure and Appl Chem 42:1147
15. Ovando-Medina VM, Martínez-Gutiérrez H, Mendizábal E, Corona MA, Peralta RD (2009) J Appl Polym Sci 111:329
16. Jovanovic R, Dubé MA (2001) J Appl Polym Sci 82:2958
17. Sajjadi S, Brooks BW (2000) Chem Eng Sci 55:4757
18. Dimitratos J, El-Aasser MS, Georgakis C, Klein A (1990) J Appl Polym Sci 40:1005
19. Delgado J (1986) Ph D dissertation, Lehigh University
20. Capek I (1999) Chem. Papers 53:332
21. Sajjadi S (2001) J Polym Sci: Part A: Polym Chem 39:3940
22. Morton M, Kaizerman S, Altier MW (1954) J Colloid Interface Sci 9:300
23. Ugelstad J, Mork PC, Mfutakamba HR, Soleimany E, Nordhuus I, Nustad K, Schmid R, Berge A, Ellingsen T, Aune O (1983) In: Poehlein GW, Ottewill RH, Goodwins JW (eds) Science and technology of polyme, vol 1.ColloidsNATO ASI Ser
24. Ledezma R, Treviño ME, Elizalde LE, Pérez-Carrillo LA, Mendizábal E, Puig JE, López RG (2007) J Polym Sci: Part A: Polym Chem 45:1463
25. Krackeler JJ, Naidus HJ (1969) Polym Sci: Part C 27:207
26. Yianneskis M (2003) Polym React Eng 11:715
27. Sajjadi S (2003) Polymer 2003 44:223
28. Plessis C, Arzamendi G, Leiza JR, Schoonbrood HAS, Charmot D, Asua JM (2003) Macromolecules 34:5147
29. Al-Bagoury M, Yaacoub EJ (2003) J Appl Polym Sci 90:2091
30. Mendizábal E, Flores J, Puig JE, López-Serrano F, Alvarez (1998) Eur Polym J 34:411
31. Rodríguez-Guadarrama LA, Mendizábal E, Puig JE, Kaler EW (1993) J Appl Polym Sci 48:775
32. Britton D, Heatley F, Lovell PA (2001) Macromolecules 34:817
33. Kong XZ, Pichot C, Guillot J (1988) Eur Polym J 24:485